ISSN (Online): 2583-7052

International Journal of Advanced Trends in Engineering and Management (IJATEM)
Vol. 03 (11), November 2024, pp. 16-32

A Streamlined Vgg-19 Classification Model for Multi-Crop Leaf Disease Prediction

D. Karthikeyan[1,*]

[1]Assistant professor, Department of Electrical and Electronics Engineering, SRM Institute of Science and Technology, Kattankulathur, Chennai, India. karthikd@srmist.edu.in

ABSTRACT

Every country economy is depending heavily on agriculture because it produces crops. Identifying leaf diseases is one of the most crucial parts of keeping a country that is agriculturally advanced. Artificial intelligence (AI) in agriculture has emerged as the most significant application in recent years. An early prediction of the type of disease affecting the plant leaves is an essential objective. To classify the current diseases type and distinguish between healthy and infected leaves, the proposed study mainly employs the Visual Geometry Group (VGG-19) classification model. The features extraction of images using a wavelet transform for extracting the features of the leaves. The model is trained and evaluated using the Apple Leaf Disease Symptoms dataset, and the adaptive wiener filter is used to enhance the images and remove noise from the leaf images, while the k-means clustering algorithm divides the regions in the leaf images. Accuracy, sensitivity, specificity, recall, and F1-score were among the performance measure parameters that were computed and tracked. This classifier is implemented using the python software. The findings show that it offers greater accuracy and the results are then contrasted with those of earlier classification methods. By identifying plant illnesses early and implementing the right treatment, this approach aims to assist farmers in protecting resources and avoiding financial loss.

Keywords: Visual Geometry Group (VGG), wiener filter, k-means clustering, wavelet transform

1 Introduction

Plants are a basic source of food for both human and animal species and agriculture is associated directly with the economic system of different countries as well. Plant health is vulnerable to bacterial and viral illnesses, just like human health [1]. Plant diseases not only jeopardize global food security but also seriously impair small farmers whose livelihoods rely on growing high-quality crops. Over 80% of all agricultural production comes from smallholder farmers, while over 50% of losses are caused by pests and diseases [2]. Due to human error, traditional disease detection methods that rely on chemical analysis of infected areas or physical inspection of sick leaves using visual signals are susceptible to low dependability and limited detection efficacy [3]. In order to improve agricultural productivity, a system that is autonomous, quick, accurate, and efficient is required to identify plant diseases and stop their spread [4].

International Journal of Advanced Trends in Engineering and Management (IJATEM)
Vol. 03 (11), November 2024, pp. 16-32

There are numerous computer-aided diagnostic (CAD) systems designed to assist farmers. These methods enhance precision, effectiveness, and impartiality of the diagnostic procedure while successfully addressing current issues. Deep learning (DL) methods have shown great promise in this area, showing great promise for data analysis and image processing [5]. Accurately classifying each pixel in a crop image into one of three categories—plant, disease, or background is the goal of agricultural segmentation. The regions of the disease classes are identified as Regions of Interest (RoI) in crop images because accurate disease region detection is essential for intelligent agricultural management [6]. One of the most important fields where classification models are thought to be useful is image and object detection. Such models are trained to detect data within images and classify them according to patterns evident in the underlying characteristics. It has been demonstrated that deep learning works well for identifying crop diseases in crops including grapes, tomatoes, and potatoes [7-8]. By feeding training datasets through optimization functions to generate strong descriptive features and carry out identification tasks based on those features, classification models have a more representational capacity than standard computer vision techniques. [9]. The machine learning agricultural systems learning methods, which entail completing a specific task using the training data and provide strategies. The model assumes that the data need to be tested following the successful completion of the training phase [10-12]. This is accomplished by collecting heterogeneous data from several sources, including soil parameters, plant canopy, climatic data, vegetation indices from remote sensing images, and Internet of Things data. Well-known machine learning methods for processing agricultural data include Support Vector Machine (SVM), Decision Tree, Random Forest, k-Nearest Neighbor (kNN), Artificial Neural Network (ANN), Principle Component Analysis (PCA), Naive Bayes, Logistic Regression, and k-mean Clustering [13-15]. In this work, proposed a streamlined leaf disease prediction for multi-crops aimed at detecting leaf images related to leaf disease, using an advanced machine learning method using VGG_19 classifier.

The proposed process of predicting leaf disease is used the leaf image dataset which contains the leaf image dataset with healthy and disease leaves. The leaf images are improved and noise removed for additional processing using an adaptive wiener filter. This method is cooperate with the k-means clustering and VGG-19 classification model for segmenting and classifying the leaf images. Using the wavelet transform feature extraction method, the suggested model additionally extracts the important aspects of an image. Metrics including accuracy, precision, sensitivity, F1-score, and specificity are used to evaluate how well transfer learning is working.

2 Related Works

Naureen Zainab *et al*. (2023) [16] have presented a method includes conversion of the image, size reduction of the image, augmenting the image, and the use of DenseNet-121. This model offers practical advice for managing and preventing illness. It also detects and categorizes the change in time in the affected area of diseased citrus leaves and detects and classifies the growth

International Journal of Advanced Trends in Engineering and Management (IJATEM)
Vol. 03 (11), November 2024, pp. 16-32

rate of citrus canker based on six distinct phases. Moreover, this method provides potential loss of important features which can lead to poor convergence and over fitting.

Abdus Salam *et al.* (2024) [17] have developed an efficient smartphone application for employing mulberry leaf disease recognition. The explainable AI (XAI) approach with a modified deep learning architecture used to appropriately classify mulberry leaves. The interpretative Grad-CAM visualization images match sericulture evaluations by experts, validating the model's predictions. This work proved with slightly lower accuracy and provide limitations on multiple datasets.

Aisha Ahmed AlArfaj *et al.* (2023) [18] have employed both the UNET approach and the learning method called Inception V3. A thorough examination of the pepper bell leaf disease dataset is the first step in this study. By using leaf images, a learning model named InceptionV3 demonstrates accuracy in distinguishing between healthy and bacterially infected pepper bell plants. In datasets with non-linear decision limits, this strategy has trouble correctly identifying the underlying patterns.

Nirmala Paramanandham *et al.* (2024) [19] have proposed an impressive advancement in agricultural science a strong deep learning-based framework for accurate diagnosis of groundnut leaf disease. An innovative framework for deep learning with the integration of residual connections and Xavier weight initialization for improved learning capabilities, LeafNet was created especially for the detection of illness in groundnut leaves. Employed both Cross Entropy Loss and Focal Loss during training to optimize performance, alongside extensive parameter tuning to fine-tune performance of the LeafNet. It showcased the classification results with lower accuracy and also have more loss on validation.

Zhiyong Xiao *et al.* (2023) [20] have proposed Important considerations in the machine learning-based leaf disease detection method are the lesions distribution and the region of interest's size. The suggested SE-VRNet combined a deep variant residual network (VRNet) with an attention mechanism and a squeeze-and-excitation (SE) module. This demonstrates the viability and efficacy of the suggested SE-VRNet in using mobile devices to identify leaf diseases. This module struggles with retaining essential information from independent input features.

3 Proposed Work

In this work, the input leaf image dataset undergoes pre-processing to enhance the image quality and remove the noise using the adaptive linear filter. Sub sequentially in the k-means clustering segmentation stage, the observed data from the leaves are thoroughly analysed to accurately describe plant, disease and background. After segmentation, In order to obtain the features of the leaf images, the wavelet transform is employed in the feature extraction procedure. Following segmentation, the classification performs using VGG-19 classification model to classifying the diseases for the leaves with better prediction accuracy.

International Journal of Advanced Trends in Engineering and Management (IJATEM)
Vol. 03 (11), November 2024, pp. 16-32

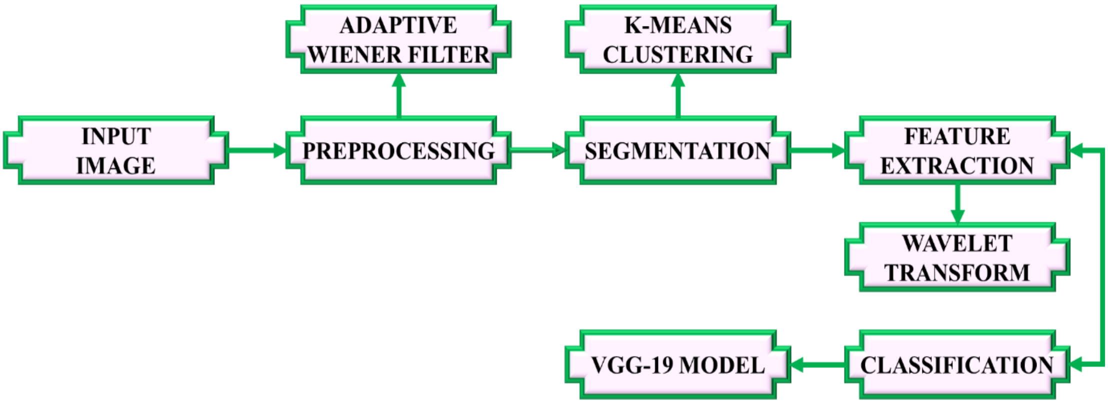

Figure 1: *Block diagram for the proposed model*

In order to determine how effective the suggested model is, a performance matrix also assesses parameters including accuracy, precision, F1-score, and recall value. This model has been built using an open-source Python platform to forecast various crops leaf diseases. The suggested model's intricate construction is seen in Figure 1.

3.1 Image Pre-processing By Adaptive Wiener Filter

The Wiener filter achieves the best possible balance between noise smoothing and filtering. It simultaneously eliminate blurring inputs and additional noise. Compared to a similar linear filter, the adaptive filter is more selective, maintaining an image borders and other high-frequency areas. The following statement describes how an adaptive wiener filter successfully suppresses Additive White Gaussian Noise (AWGN) in digital images:

$$f(i,j) = m + \frac{1^2-\sigma^2}{\sigma^2}(I(i,j) - m) \quad (1)$$

I =Pixel intensity locating in the $i-th$ row and the $j-th$ column of the input image, $J =$ the pixel intensity of the output image, σ^2=noise variance of input image, $m =$ local mean, mask $= k,\ P \times Q$ =size of the pixels

$$m = \frac{1}{PQ}\sum_{i,j\in k} I(i,j) \quad (2)$$

The variance is found from:

$$t^2 = \frac{1}{PQ}\sum_{i,j\in k} I^2(i,j) - m^2 \quad (3)$$

For each location in the mask, the filter employs the mean of the local variances if σ^2 is unknown. This is a serious drawback to the Wiener filter processing concept, both computationally and in terms of the filtered image quality. To overcome this limitation approximation of noise variance is calculated. An estimate of the noise variance from an unidentified image is shown below. When the noise is regarded as additive, the vector form of the following equation applies for a specific square area of the image:

International Journal of Advanced Trends in Engineering and Management (IJATEM)
Vol. 03 (11), November 2024, pp. 16-32

$$I(i_0, j_0) = I_0(i_0, j_0) + n(i_0, j_0) \tag{4}$$

$I =$ Area of noise image at centre $(i_0, j_0)$the pixel, I_0= original area content, $n =$ same zone noise, $v =$ unit vector

$$var(v^T I) = var(v^T I_0) + \sigma^2 \tag{5}$$

$var\{.\} =$ approximation of variance. Using the corresponding direction, the set of tested directions showed the least amount of variance. v_{min}= minimal eigenvalue of the covariance matrix.

$$K_I = \frac{1}{N} \sum_{N=1}^{N^2} (I - m)(I - m)^T \tag{6}$$

$N =$ Number of regions analyzed in both vertical and horizontal directions.

$$\lambda_{min}(K_I) = \lambda_{min}\left(K_{I_0}\right) + \sigma^2 \tag{7}$$

$\lambda_{min} =$ Minimum eigenvalue of the associated matrix of covariance. When a comparatively homogeneous portion of the image is subjected to equation (7),

$$\lambda_{min}(K_{I_0}) \approx 0 \tag{8}$$

Then the approximated variance will be:

$$\tilde{\sigma}^2 = \lambda_{min}(K_I) \tag{9}$$

By computing the covariance matrix of the gradient map from each tested zone, the maximal eigenvalue is chosen, and the eigenvectors and eigenvalues of the gradient map are computed. If the eigenvalue is less than a threshold determined through iterative testing, the area is deemed flat, and the approximate noise variance is estimated. For subsequent processing, this technique improves and lowers the noise in the leaf image.

3.2 Image Segmentation by K-Means Clustering

Image segmentation is the basic approach used for the digital conversion of the leaf image into multiple distinct regions. In this study, k-means clustering has been utilized to create segmented masks from image segmentation and categorize them. Here, two clusters are subjected to k-means clustering in order to create the divisions. where images with normal findings are found in the first cluster, whereas problematic results are found in the second cluster. The main rule considered here is the variety of category feature set. Using the data points, the iterative technique calculates the centroid by calculating the Euclidean distance from the original cluster. Finding the cluster centroid over the defined clusters is done using this distance.

The clustering approach is the process of organizing images based on specific characteristics. It is necessary to cluster both infected and un-diseased images. Clustering involves removing the background from HSV images, reducing features like brightness and darkness, and inserting only colored images for evaluation. The image is divided into four groups, for

International Journal of Advanced Trends in Engineering and Management (IJATEM)
Vol. 03 (11), November 2024, pp. 16-32

example, if four clusters are found, yielding a decent image segmentation result. The performance of the K-means clustering technique is shown in Figure 2.

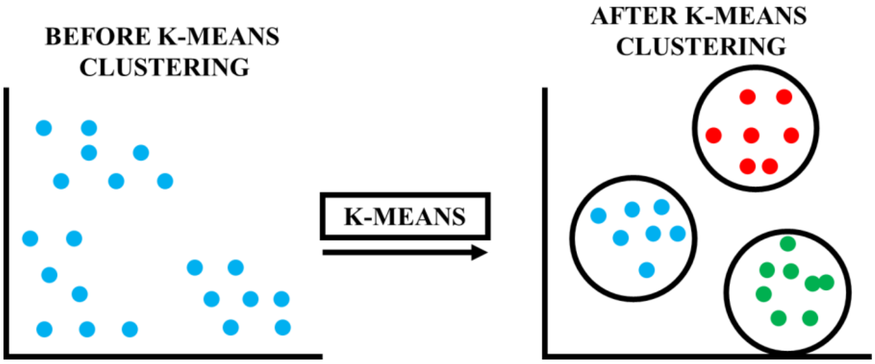

Figure 2: *Functionality of K-means clustering*

The Euclidean distance and center of each leaf-based pixel are calculated as follows, and the number of clusters needs to be initialized:

$$d = p_x^y - C_k \tag{10}$$

d =Euclidean distance, p_x^y = clustered input pixel, C_k = center of the cluster
Depending on the distance, assign each pixel to the closest center. The new position is then determined using the particular expression.

$$C_k = \frac{\sum_{y \in C_k} \sum_{x \in C_k} p_x^y}{N} \tag{11}$$

The leaf is segmented and used for feature extraction after repeating till the error value is computed and the relevance of the image is plotted.

3.3 Feature Extraction by Wavelet Transform

Information is possible to extract from a wide variety of data types using wavelet transform. Wavelet transform's time-frequency localization feature has led to its recent widespread use in signal and image processing. Every analytic wavelet has a unique frequency band, time duration, and time location. To extract the important characteristics from improved leaf samples, the Wavelet Transform is employed. The wavelet transform breaks down into sub-bands of lower components, including approximation (LL), horizontal (LH), vertical (HL), and higher frequency components, such as diagonal (HH). When compared to the wavelet transform's higher frequency components, the LL component contains the most information. The wavelet-scale evolution of the energy from the calculation of specific steps has the following characteristics:
According to the aforementioned wavelet transform techniques, the curve spectrum represents the scale wavelet.

International Journal of Advanced Trends in Engineering and Management (IJATEM)
Vol. 03 (11), November 2024, pp. 16-32

$$S_k(t), k = 1,2, \ldots \ldots, K \tag{12}$$

For every wave energy sub-scale

$$E(k) = \int |S_k(t)|^2 \, dt \quad 13)$$

Wavelet energy normalized

$$T(k) = \frac{E(k)}{\sum_{k=1}^{K} E(k)} \tag{14}$$

Energy normalization for the discrete cosine transform (DCT), which is comparable to the KL transform, need to eliminate redundancy in order to play a meaningful function.

$$c(n) = w(n) \sum_{k=1}^{K} T(k) cos \frac{\pi(2k-1)(n-1)}{2K}, n = 1,2, \ldots \ldots, M \tag{15}$$

In which

$$w(n) = \begin{cases} \sqrt{\frac{2}{K}}, 2 \leq n \leq M \\ \frac{1}{\sqrt{K}}, n = 1 \end{cases} \tag{16}$$

Taking $c(n), n = 2,3, \ldots L, M$ in the rear of the experiment classification. For unsupervised clustering, L, M is a $M - 1$ dimensional feature vector. The following are the most popular texture-based features. Sum of squares, variance, homogeneity, autocorrelation, dissimilarity, and entropy. In order to detect and categorize the images, the classifiers use the feature vectors created by combining the wavelet transform features.

3.4 Classification by Visual Geometry Group (Vgg-19)

The CNN VGG-19 transfer learning model has 19 layers, 16 convolutional layers, and 3 thick layers, and it is capable of dividing images into 1000 different categories. Three fully connected (FC) layers, two Conv 1 max pools, four Conv 1 max pools, and two Conv 1 max pools make up the model. ConvNets are a popular model for image prediction since they incorporate many 3 x 3 filters.

DL networks, which have about 60 million parameters and 650,000 neurons, are used for image categorization in many different disciplines using enormous datasets. Five convolutional layers and three fully connected layers with various purposes make up the actual network architecture. The standard and max-pooling layers are the first two convolution layers; the output layer is the softmax layer; the third and fourth convolution layers are directly connected; and the final convolution layer is the max-pooling layer. Moreover, a number of networks have particular configurations for certain applications. To give one example, Google Net has eight inception modules, four convolutional layers, four max-pooling layers, three average pooling layers, five fully connected layers, three softmax layers, and almost seven million parameters. All convolutional and dropout layers employ the ReLU (activation function), and all fully

International Journal of Advanced Trends in Engineering and Management (IJATEM)
Vol. 03 (11), November 2024, pp. 16-32

connected layers undergo a 70% parameter reduction ratio. Similar to VGG-19, ResNet has undergone numerous modifications to create ResNet-18, ResNet-34, ResNet-50, ResNet-101, and ResNet-152. Here, the multi-crop leaf image dataset is trained using VGG-19.

One of the VGG-based architectures is VGG-19; in essence, VGG is a CNN network architecture. Three fully connected layers and sixteen convolution layers make up the 19 connection layers of the VGG-19 model. The fully linked layers will classify the leaf images based on those features, but the max-pooling layers will minimize the features and prevent overfitting, as shown in figure 3.

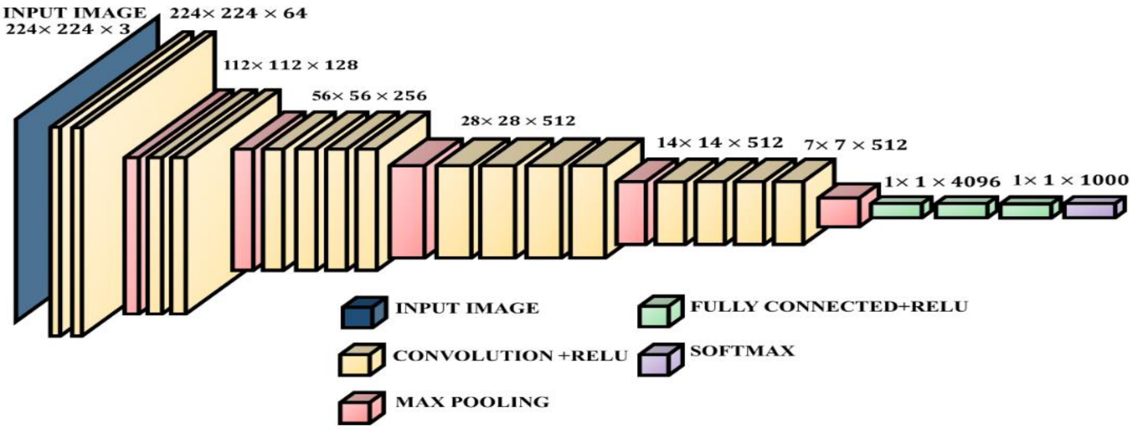

Figure 3: *An overview of the VGG-19 architecture*

The output of each convolutional layer is denoted by the expression:

$$C_j^l = \varphi(\sum_{i=1}^{M^{l-1}} C_i^{l-1} \times k_{ij}^l + b_j^{l-1} \qquad (17)$$

b_j = bias value, φ = activation function

In the $(l-1)$th, lth layers, the convolutional function $\times$ is used to represent the relationship between the weights of the i^{th} and j^{th}features.

To retrain the other objects, DL networks frequently employ transfer learning from the trained item. Transfer learning is often divided into four categories: case, features, parameter, and relationship based learnings. Naturally, it is very challenging to choose the training settings for the best classification system. In this case, the network parameters and an appropriate network architecture has to be addressed, and these values have to be calculated with the updated input data. The recently launched network is then modified to improve performance. This study used the parameter-based transfer learning approach to classify leaf diseases in a number of crops. To improve categorization, the VGG-19 network will specifically freeze the convolution layers and retrain the fully connected layers. By altering the learning rate, epoch, and batch size, this also selects the optimal network.

International Journal of Advanced Trends in Engineering and Management (IJATEM)
Vol. 03 (11), November 2024, pp. 16-32

3.5 Predicted Performance Matrix

A number of fundamental indicators are taken into account in the experimental evaluation that follows, including TP (True Positive), TN (True Negative), FP (False Positive), and FN (False Negative).TP stands for attack flows that were correctly anticipated, TN for normal flows that were correctly predicted, FP for attack flows that were mistakenly predicted, and FN for normal flows that were incorrectly predicted.

3.5.1 Accuracy

The ratio of correct guesses to total predictions is used to calculate accuracy. A higher accuracy means that the learning model is making more accurate predictions and it is mentioned as

$$Accuracy = \frac{TP+TN}{TP+FP+TN+FN} \tag{18}$$

3.5.2 Precision

A high precision rate is equal to a low rate of false positives, which can be prevented by not misclassifying negative records as positive. It is the percentage that accurately predicted every attack that was anticipated, as shown by

$$Precision = \frac{TP}{TP+FP} \tag{19}$$

3.5.3 Recall

Recall, also known as the true positive rate, is the proportion of accurately predicted attacks to actual attacks, and it is shown by

$$Recall = \frac{TP}{TP+FN} \tag{20}$$

3.5.4 F1 score

Averaging precision and recall yields the F1 score, which is

$$F1\ score = \frac{2.(Recall.Precision)}{Recall+Precision} \tag{21}$$

3.5.5 AUC

The Area under the ROC Curve (AUC) illustrates the Recall against False Positive Rate at different categorization criteria.

$$FPR = \frac{FP}{FP+TN} \tag{22}$$

The module makes predictions for the categorized datasets and assesses the confusion matrix, accuracy, recall, time, F1 score, and precision. At last, the classification technique's performance is attained.

International Journal of Advanced Trends in Engineering and Management (IJATEM)
Vol. 03 (11), November 2024, pp. 16-32

Article Title: A Streamlined Vgg-19 Classification Model for Multi-Crop Leaf Disease Prediction

4 Results and Discussions

This classification implementation of the model using the Python platform. A dataset containing instances of both healthy and diseased leaves is necessary for training a model for classifying leaf diseases. This proposed model used the Apple Leaf Disease Symptoms Dataset for testing and training process. 480 images were gathered for training and testing, respectively. 80 percentage of the data is used to train the model existed in one set of labelled images, while 20 percentage is in the other set used for testing or validation. The illnesses that damage apple leaves and are included in the dataset are apple-black rot, apple-ceder rust, and apple-scab.

```
Train Classes and Image Counts:
Apple_black_rot: 136
Apple_cedar_rust: 128
Apple_scab: 120
Total Train Images: 384

Test Classes and Image Counts:
Apple_black_rot: 34
Apple_cedar_rust: 32
Apple_scab: 30
Total Test Images: 96

Total Images (Train + Test): 480
```

Figure 4: *Total Dataset Images Count*

Figure 4 displays the chosen leaf images for additional processing, and Figure 5 shows the distribution of images for each class, including apple-black-rot, apple-ceder-rust, and apple-scab. Figure 6 presents representative images of apple leaves for each class in order to illustrate the leaf disease classification method.

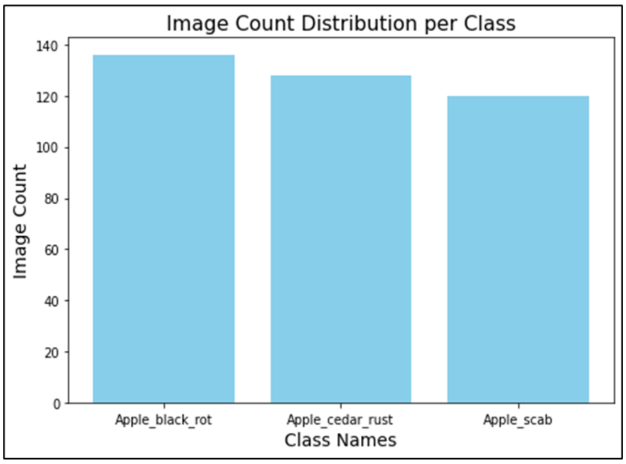

Figure 5: *Image count for all the classes*

International Journal of Advanced Trends in Engineering and Management (IJATEM)
Vol. 03 (11), November 2024, pp. 16-32

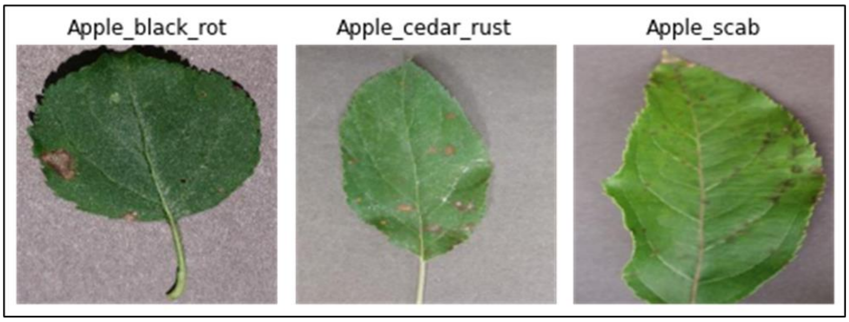

Figure 6: *Sample Class Images*

To predict illness, images of leaves are employed. Resizing changes the pixel count of the images, which affects the amount of information needed to explain the image as well as its visual size. Following resizing, the images are transformed into grayscale for additional processing. In order to remove blur from grayscale images caused by linear motion or unfocused optics, preprocessing is conducted using the Wiener filter. After that, segmentation is applied to the previously processed image. The leaf images are segmented using the K-means clustering technique, which determines various classes or clusters within the supplied leaf image based on the image's degree of similarity. Figure 7 displays the processing operations performed on the given leaf image dataset.

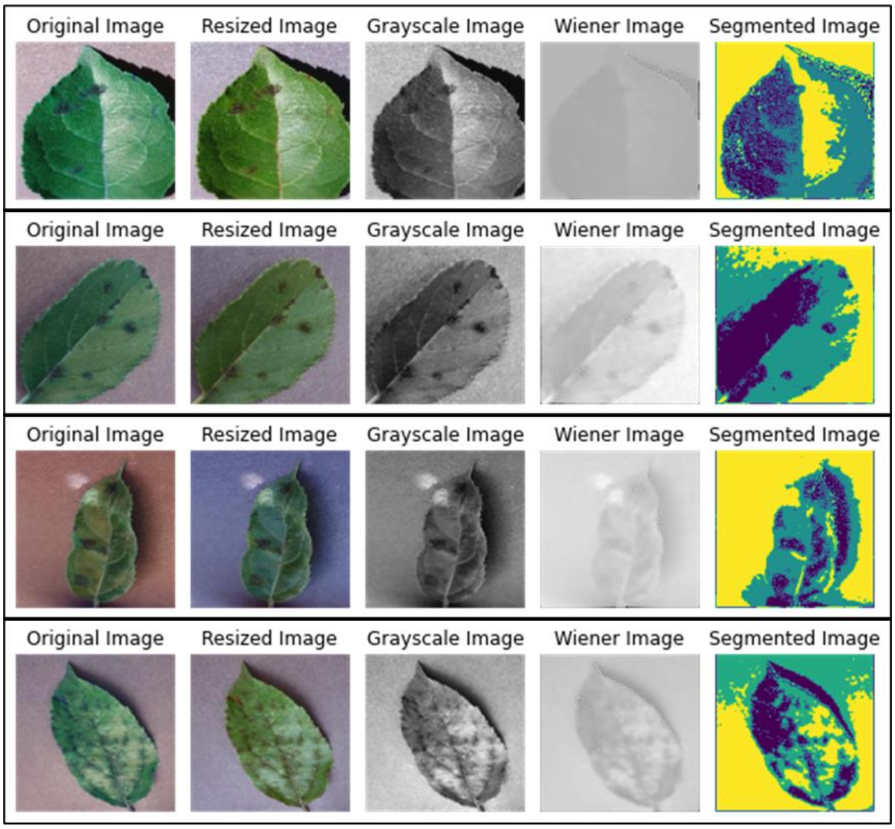

Figure 7: *Image Processing Stages on leaf images*

International Journal of Advanced Trends in Engineering and Management (IJATEM)
Vol. 03 (11), November 2024, pp. 16-32

The useful information is extracted from the enhanced leaf images using the wavelet transform. It broke down into sub-bands with higher frequency (HH) and lower frequency (LL, LH, and HL) components. The DWT breaks down into sub-bands of higher frequency components like diagonal (HH), horizontal (LH), vertical (HL), and lower components like approximation (LL). Figure 8 shows the segmented leaf images using the wavelet transform.

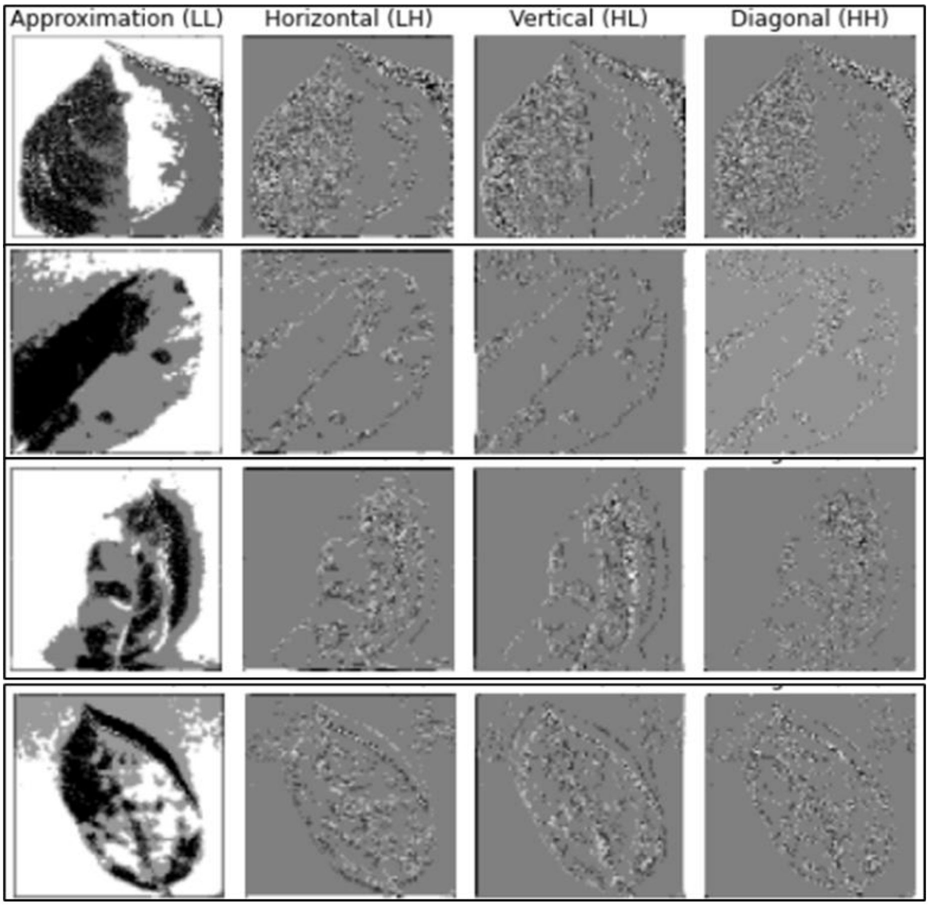

Figure 8: *Feature Extraction by Wavelet Transform Coefficient*

The effectiveness of the suggested method is assessed by measuring and validating a model's performance on apple leaves. It validated the loss function on these datasets and compared the model's performance on the training and validation datasets. The accuracy and VGG-19 loss throughout training and validation using the apple leaf disease symptom dataset are displayed in Figure 9. The results show that this model performed well on both sets. More specifically, on the Apple dataset, it achieved a 96% accuracy rate with the least amount of loss for both the training set and validation set.

International Journal of Advanced Trends in Engineering and Management (IJATEM)
Vol. 03 (11), November 2024, pp. 16-32

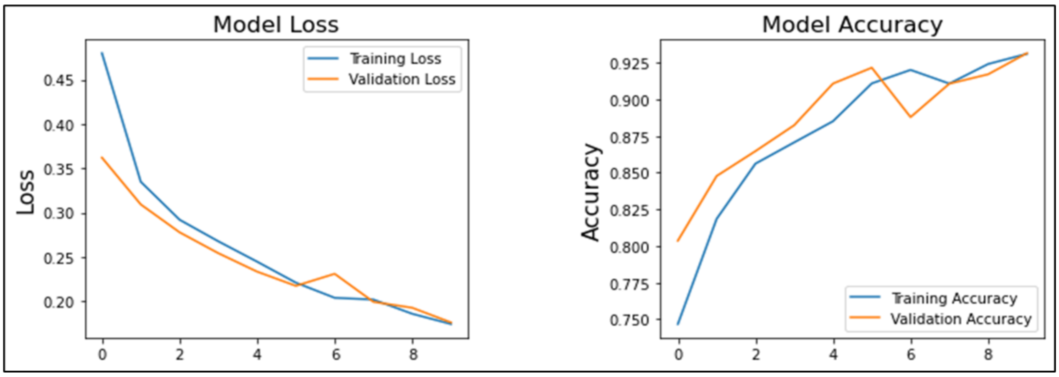

Figure 9: *Model loss and accuracy*

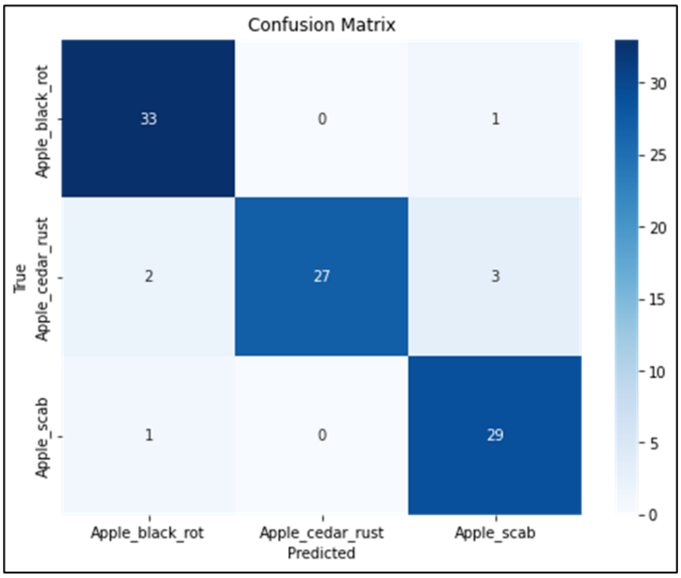

Figure 10: *Confusion matrix for the proposed model*

A VGG_19 classification model was used to create a two-column matrix that included all true positives, false positives, true negatives, and false negatives. Figure 10 illustrates how the performance parameter for apple leaves has been measured using the confusion matrix. Test approximately with the information gathered. The apple leaf disease symptoms dataset, which were captured in a real-world setting with a range of backgrounds and light levels, are used to test the proposed method.

International Journal of Advanced Trends in Engineering and Management (IJATEM)
Vol. 03 (11), November 2024, pp. 16-32

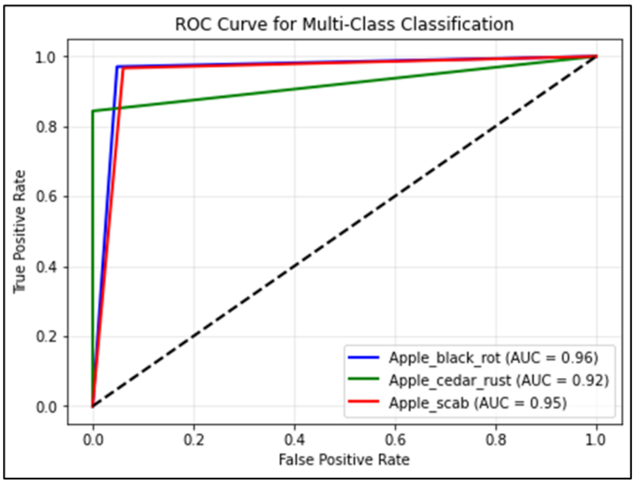

Figure 11: *ROC curve for multi-class classification*

Plotting the results of the rates of true positive and false positive in receiver operating characteristics (ROC) curves, which are graphs that display the performance of the VGG-19 classifier. It shows statistical accuracy of the classifier, whereas figure 11 shows the ROC curve for each class.

Classification Report:

	precision	recall	f1-score	support
0	0.92	0.97	0.94	34
1	1.00	0.84	0.92	32
2	0.88	0.97	0.92	30
accuracy			0.93	96
macro avg	0.93	0.93	0.93	96
weighted avg	0.93	0.93	0.93	96

Figure 12: *Performance Matrix*

By examining the performance matrices, the proportion of accurate forecasts to total predictions is determined. The precision, recall, F1 score, and accuracy are computed based on the anticipated leaf illness. The computed assessed values are shown in Figure 12.

ISSN (Online): 2583-7052

International Journal of Advanced Trends in Engineering and Management (IJATEM)
Vol. 03 (11), November 2024, pp. 16-32

Article Title: A Streamlined Vgg-19 Classification Model for Multi-Crop Leaf Disease Prediction

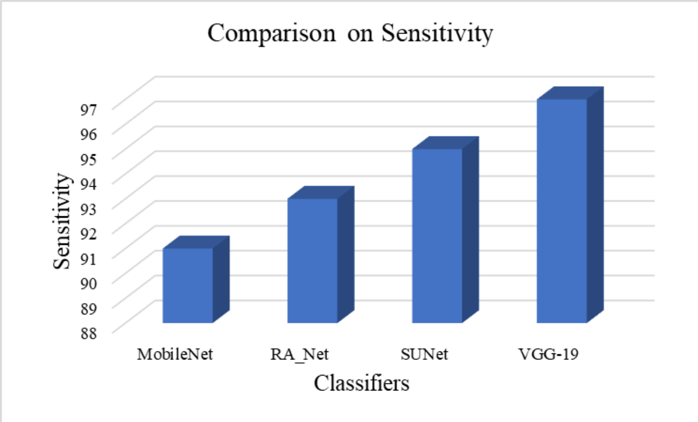

Figure 13: *Comparison graph for sensitivity with other methods*

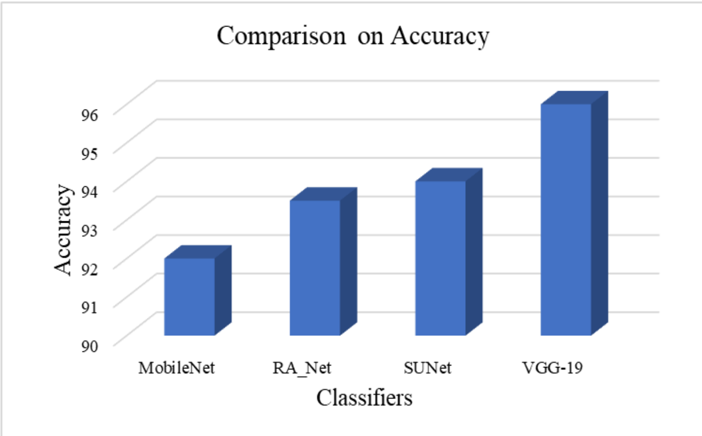

Figure 14: *Comparison graph for accuracy with other methods*

Figure 13 and figure 14 shows the sensitivity and accuracy of various classifiers in which the proposed classifier shows the highest specificity of 97 % and accuracy of 96% than other classifiers such as Mobile Net [3], Rot Attention Network (RA_Net)[5] and SUNet[7].

5 Conclusion

One important and difficult issue in global agriculture is the identification and classification of plant and leaf diseases. The VGG_19 classification model was used in this investigation to determine the cause of leaf disease. Pre-processing and segmentation played a vital role to enhance the leaf image for getting better efficiency on further processing. All the processing steps are conducted with the Apple Leaf Disease Symptoms dataset. The suggested model is constructed and tested to enhance the performance that is reviewed and contrasted, and it successfully detects leaf disease with an improved accuracy rate of 96%. The performance of the classification model is evaluated using the metrics of accuracy, precision, recall, and F1-score. The precision value was 92%, the recall value was 97%, and the F1-score was 94%. When compared to other available data sets and methodologies, the evaluation metrics

International Journal of Advanced Trends in Engineering and Management (IJATEM)
Vol. 03 (11), November 2024, pp. 16-32

parameters are larger and more thorough. As a result, the suggested approach outperformed previous studies on plant leaf disease in terms of symptom severity estimation. A localization technique for determining the diseased leaf area will be developed in the future.

References

1. Ammar Oad; Syed Shoaib Abbas; Amna Zafar; Beenish Ayesha Akram; Feng Dong; Mir Sajjad Hussain Talpur, Year: 2024, "Plant Leaf Disease Detection Using Ensemble Learning and Explainable AI", IEEE Access, Vol: 12, pp. 156038 – 156049.

2. R. Kavitha Lakshmi; Nickolas Savarimuthu, Year: 2021, "PLDD-A Deep Learning-Based Plant Leaf Disease Detection", IEEE Access, Vol: 11, pp. 44 – 49.

3. Sabbir Ahmed; Md. Bakhtiar Hasan; Tasnim Ahmed; Md. Redwan Karim Sony; Md. Hasanul Kabir, Year: 2022, "Less is More: Lighter and Faster Deep Neural Architecture for Tomato Leaf Disease Classification", IEEE Access, Vol: 10, pp. 68868 – 68884.

4. Zhiyan Liu; Rab Nawaz Bashir; Salman Iqbal; Malik Muhammad Ali Shahid; Muhammad Tausif; Qasim Umer, Year: 2022, "Internet of Things (IoT) and Machine Learning Model of Plant Disease Prediction–Blister Blight for Tea Plant", IEEE Access, Vol: 10, pp. 44934 – 44944.

5. Natasha Nigar; Hafiz Muhammad Faisal; Muhammad Umer; Olukayode Oki, Jose Manappattukunnel Lukose, Year: 2024, "Improving Plant Disease Classification With Deep-Learning-Based Prediction Model Using Explainable Artificial Intelligence", IEEE Access, Vol: 12, pp. 100005 – 100014.

6. Goo-Young Moon; Jong-Ok Kim, Year: 2024, "RoI-Attention Network for Small Disease Segmentation in Crop Images", IEEE Access, Vol: 12, pp. 63725 – 63734.

7. Deepak Thakur; Tanya Gera; Ambika Aggarwal; Madhushi Verma; Manjit Kaur; Dilbag Singh, Year: 2024, "SUNet: Coffee Leaf Disease Detection Using Hybrid Deep Learning Model", IEEE Access, Vol: 12, pp. 149173 – 149191.

8. Kamlesh S Patle; Riya Saini; Ahlad Kumar; Vinay S. Palaparthy, Year: 2021, "Field Evaluation of Smart Sensor System for Plant Disease Prediction Using LSTM Network", IEEE Access, Vol: 22, pp. 3715 – 3725.

9. Changjian Zhou; Zhiyao Zhang; Sihan Zhou; Jinge Xing; Qiufeng Wu; Jiaz Song, Year: 2021, "Grape Leaf Spot Identification Under Limited Samples by Fine Grained-GAN", IEEE Access, Vol: 9, pp. 100480 – 100489.

10. Riya Saini; Kamlesh S. Patle; Ahlad Kumar; Sandeep G. Surya; Vinay S. Palaparthy, Year: 2022, "Attention-Based Multi-Input Multi-Output Neural Network for Plant Disease Prediction Using Multisensor System", IEEE Access, Vol: 22, pp. 24242 – 24252.

International Journal of Advanced Trends in Engineering and Management (IJATEM)
Vol. 03 (11), November 2024, pp. 16-32

11. Vasileios Balafas; Emmanouil Karantoumanis; Malamati Louta; Nikolaos Ploskas, Year: 2023, "Machine Learning and Deep Learning for Plant Disease Classification and Detection" IEEE Access, Vol: 11, pp. 14352 – 114377.

12. Kamlesh S. Patle; Neha Sharma; Priyanka Khaparde; Harsh Varshney; Gulafsha Bhatti; Yash Agrawal, Year: 2024, "Impact of Electrode Patterns Variation on the Response Characteristic of Leaf Wetness Sensors", IEEE Access, Vol: 2, pp. 536 – 544.

13. Uferah Shafi; Rafia Mumbai; Muhammad Deedahwar Mazhar Qureshi; Zahid Mahmood; Sikander Khan Tanveer; Ihsan Ul Haq, Year: 2023, "Embedded AI for Wheat Yellow Rust Infection Type Classification", IEEE Access, Vol: 11, pp. 23726 – 23738.

14. Mamunur Rashid; Bifta Sama Bari; Yusri Yusup; Mohamad Anuar Kamaruddin; Nuzhat Khan, Year: 2021, "A Comprehensive Review of Crop Yield Prediction Using Machine Learning Approaches With Special Emphasis on Palm Oil Yield Prediction", IEEE Access, Vol: 9, pp. 63406 – 63439.

15. Yafeng Zhao; Zhen Chen; Xuan Gao; Wenlong Song; Qiang Xiong; Junfeng Hu, Year: 2021, "Plant Disease Detection Using Generated Leaves Based on DoubleGAN", IEEE Access, Vol : 19, pp. 1817 – 1826.

16. Naureen Zainab; Hammad Afzal; Taher Al-Shehari; Muna Al-Razgan; Naima Iltaf; Muhammad Zakria, Year: 2023, "Detection and Classification of Temporal Changes for Citrus Canker Growth Rate Using Deep Learning", IEEE Access, Vol: 11, pp. 127637 – 127650.

17. Abdus Salam; Mansura Naznine; Nusrat Jahan; Emama Nahid; Md Nahiduzzaman; Muhammad E. H. Chowdhury, Year: 2024, "Mulberry Leaf Disease Detection Using CNN-Based Smart Android Application", IEEE Access, Vol:12, pp. 83575 – 83588.

18. Aisha Ahmed AlArfaj; Abdulaziz Altamimi; Turki Aljrees; Shakila Basheer; Muhammad Umer, Md. Abdus Samad, Year: 2023, "Multi-Step Preprocessing With UNet Segmentation and Transfer Learning Model for Pepper Bell Leaf Disease Detection", IEEE Access, Vol: 11, pp. 132254 – 132267.

19. Nirmala Paramanandham; Shyam Sundhar; P. Priya, Year: 2024, "Enhancing Disease Detection with Weight Initialization and Residual Connections Using LeafNet for Groundnut Leaf Diseases", IEEE Access, Vol: 12, pp. 91511 – 91526.

20. Zhiyong Xiao; Yongge Shi; Gailin Zhu; Jianping Xiong; Jianhua Wu, Year:2023, "Leaf Disease Detection Based on Lightweight Deep Residual Network and Attention Mechanism", IEEE Access, Vol: 11, pp. 48248 – 48258.